UNCLASSIFIED

AD NUMBER
AD069214
CLASSIFICATION CHANGES
TO: **UNCLASSIFIED**
FROM: **CONFIDENTIAL**
LIMITATION CHANGES
TO: **Approved for public release; distribution is unlimited.**
FROM: **Distribution authorized to U.S. Gov't. agencies and their contractors; Administrative/Operational Use; APR 1955. Other requests shall be referred to Army Research Laboratory, Aberdeen Proving Ground, MD 21005.**
AUTHORITY
USABRL notice 15 Oct 1964; USABRL ltr, 22 Apr 1981

THIS PAGE IS UNCLASSIFIED

[redacted]

Reproduced
by the

DOWNGRADED AT 3 YEAR INTERVALS:
DECLASSIFIED AFTER 12 YEARS
DOD DIR 5200.10

[redacted]

CONFIDENTIAL

69214

BRL

FC

C-1

MEMORANDUM REPORT No. 885

Free Flight Tests Of A Model Of The 'Redstone', XSSM-A-14, Warhead

WALTER K. ROGERS, JR.

DEPARTMENT OF THE ARMY PROJECT No. 5B0303009
ORDNANCE RESEARCH AND DEVELOPMENT PROJECT No. TB3-1838

BALLISTIC RESEARCH LABORATORIES

ABERDEEN PROVING GROUND, MARYLAND

CONFIDENTIAL

CONFIDENTIAL

BALLISTIC RESEARCH LABORATORIES

MEMORANDUM REPORT NO. 885

APRIL 1955

FREE FLIGHT TESTS OF A MODEL OF THE 'REDSTONE', XSSM-A-14, WARHEAD

Walter K. Rogers, Jr.

Department of the Army Project No. 5B0303009
Ordnance Research and Development Project No. TB3-1838

ABERDEEN PROVING GROUND, MARYLAND

CONFIDENTIAL

TABLE OF CONTENTS

BALLISTIC RESEARCH LABORATORIES

MEMORANDUM REPORT NO. 885

WKRogersJr/jmc
Aberdeen Proving Ground, Md.
April 1955

FREE FLIGHT TESTS OF A MODEL OF THE 'REDSTONE', XSSM-A-14, WARHEAD

ABSTRACT

A free flight range program was conducted with 4.29% scale models of the "Redstone" XSSM-A-14 Warhead Model in the Transonic Free Flight Range. The velocity range tested was from Mach number 0.98 to 3.25. The normal and drag forces, the pitching and rolling moments and the damping in pitch and roll were measured. The results are presented in coefficient form in tables and graphs.

SYMBOLS

Symbols	Definition	Units
A	Axial moment of inertia	slugs ft^2
b_1	Precessional rate	degrees/ft
b_2	Nutational rate	degrees/ft
b	Wing span	ft
B	Transverse moment of inertia	slugs ft^2
c	Wing chord	ft
C_D	Aerodynamic drag coefficient $\frac{2D}{\rho S V^2}$	1
C_{D_f}	Fore drag coefficient	1
$C_{D_{f_{\alpha^2}}}$	Slope of fore drag coefficient versus square of angle of attack	
C_{D_0}	Aerodynamic drag coefficient at zero yaw	1
C_L	Aerodynamic lift coefficient $\frac{2L}{\rho S V^2}$	1
C_{L_α}	Slope of lift coefficient versus angle of attack	1/degree
$C_{\ell_{\delta_v}}$	Roll moment derivative due to canted surfaces $\frac{\partial C_\ell}{\partial \delta_v}$	1/rad
C_{ℓ_p}	Roll moment derivative due to rolling velocity $\frac{\partial C_\ell}{\partial \frac{pb}{2V}}$	1/rad
C_ℓ	Roll moment coefficient $\frac{L}{qA_D}$	1
C_M	Aerodynamic pitching moment coefficient $\frac{2M}{\rho S V^2}$	1
C_{M_α}	Slope of moment coefficient versus angle of attack	1/degree
$(C_{M_q} + C_{M_{\dot\alpha}})$	Damping moment derivatives	1
C_N	Aerodynamic normal force coefficient $\frac{2N}{\rho S V^2}$	1

C_{N_α}	Slope of Normal Force coefficient versus angle of attack	1/degree
d	Maximum diameter of body	1
D	Drag force	lb
H	Damping moment in pitch	ft lb
k_1	Precessional arm	rad
k_2	Nutational arm	rad
k_3	Tricyclic arm	rad
K_D	Ballistic Drag coefficient	1
K_{D_0}	Ballistic drag coefficient at zero yaw	1
K_H	Ballistic damping moment coefficient	1
K_L	Ballistic lift coefficient	1
K_M	Ballistic pitching moment coefficient	1
K_N	Ballistic normal force coefficient	1
ℓ	length of model = 4.341 d	ft
L	Lift force	lb
M	Yaw moment	ft lb
M	Mach number	1
N	Normal force	lb
p	Rolling velocity $\dot{\phi}_v$	rad/sec
pb/2V	Fin tip helix angle	rad
q	Dynamic pressure $\frac{\rho V^2}{2}$	lb/ft^2
R_e	Reynolds number $\frac{\rho V \ell}{\mu}$	1
S	Maximum frontal area of body	ft^2
S_L	Radius of lift swerving motion	ft
V	Linear velocity of missile along trajectory	ft/sec
α	Angle of attack	degree
δ	Angle between axis of missile and tangent to the trajectory	rad
δ_v	Angle of cant of vane	rad
ρ	Air density	$slugs/ft^3$
ϕ_v	Angle of roll	rad
λ_1	Damping rate of precessional arm	1/ft
λ_2	Damping rate of nutational arm	1/ft

Note: Dot above symbol indicates time derivative of variable

INTRODUCTION

"Redstone" project originally known as "Major" project is a development program for a surface-to-surface guided missile with a separating warhead. Since a high degree of accuracy and reliability is essential, the warhead must be a dynamically and statically stable configuration. At the present stage of development, the warhead is wingless with four small vanes near the base for controlled guidance. Wind tunnel tests on this configuration, conducted at Aberdeen Proving Ground, indicated that the static stability would become negative around Mach number 5, and that the overall stability picture needed clarification.

For this reason, it became necessary to determine the aerodynamic forces and moments acting on this configuration, particularly the damping in yaw and the magnitude of the roll derivatives at few Mach numbers. A free flight program involving the firing of 18 models over a Mach number range from .98 to 3.25 has therefore been conducted at BRL's Transonic Range.

Throughout the report, ballistic nomenclature is used. However, conversion formulae are given, and the tables and graphs contain both ballistic and aerodynamic nomenclature.

INSTRUMENTATION

The instrumentation used in this program was the Transonic Free Flight Range. This facility is described in some detail in reference 2. Photographs of the exterior and interior of the range are presented in figure 1 and 2 respectively. The range is an enclosed building which offers at present 680 feet of observed trajectory at twenty-five photographic stations. The medium of spark photography is employed. The spark light sources are of about two microseconds in duration. Spark interval time pulses can be recorded by 1.6 megacycle counters at 16 of the stations. The surveyed distances in the range have an overall data accuracy of about .01 ft and angular measurements of yaw are good to about 6 minutes of arc. The records obtained at each station on this program are shown in figures 3, 4, and 5. The fiducial system may be seen on these records in the form of a wire to which all distance and angle measurements are referred. For every missile launched at least one direct photograph is taken to determine the flight condition of the model. An example may be seen in figure 6.

MODELS

The models were scaled from sketches furnished by Redstone Arsenal and were designed specifically for free flight testing in the Transonic Range.[1]

---

[1] The author is indebted to Mr. Richard Sager, formerly with BRL, for his work on the design of the models and sabots for this program and to Mr. Oscar Holderer, Redstone Arsenal, for suggestions concerning certain details of design of the models.

The model appears in sketch 1 and in figure 8. The scale was 4.29% which gave a maximum base diameter of 3 inches (excluding vanes). The model was designed for launching from a smooth bore, 6.2 inch, tank mounted gun, see figure 1. A bronze nose section and magnesium afterbody with duraluminum vanes were used to place the center of gravity at 2.23 calibers from the base. A permanent magnet was incorporated to furnish the necessary triggering pulse for the spark stations in the range. The physical measurements of the models are averaged as follows:

Axial moment of inertia, A 0.0355 lb. ft^2

Transverse moment of inertia, B, 0.490 lb. ft^2

Center of gravity, distance from base, 6.697 inches or 2.23 cal.

Weight - 2818 grams

Wing span, b, 0.3725 ft.

Wing Chord, c, 0.0518 ft.

Body length, ℓ, 1.0853 ft.

Four of the models had nominal 2 degree canted vanes to induce rolling motion.

The most difficult problem in the entire program arose in the design of a sabot capable of successfully launching the model at fairly high velocities through a blast shield port and into the enclosed range proper. The sabot, in addition to protecting the model from the gun and the powder gases, and launching the model at the desired attitude had another stringent requirement: it must break up or separate in some fashion and not enter the range proper. Obviously, high velocity particles from such sabots can do extensive damage to range equipment if allowed to enter the instrumented range. After some rather painful experience, the sabot as seen in sketch 2 and photographs, figure 9 a, b was designed and was fairly successful. It might be noted that the model was canted in the sabot at 2 degrees to the axis. This was done on nearly all of the program firings for two reasons: first, it was desirable to cause yaw of from one to six degrees in order to obtain greater relative accuracy of measurement of the yawing motion and still be within the assumptions of the linearized theory; second, it has been found from experience that in order to avoid having the rather heavy base material from the sabot enter the range, proper orientation between the canted model and the gun aiming point is necessary.

Reference 5 gives a more detailed discussion of the sabot problem in general. In figure 7, a series of frames taken by 8 x 16 mm Fastax Cameras, at about 12000 frames/sec, show the launching sequence of one of the warhead models.

DATA REDUCTION

The range records in the form of photographic plates, timing data, and atmospheric conditions in the range were processed by the Data Reduction Section to calculate the aerodynamic forces and moments. This reduction of the Spark Range data is described thoroughly in Ref. 3.

The standard procedure for obtaining the dependence of drag coefficients on the magnitude of yaw could not be used in this program since not enough models were fired at any one velocity to allow a good determination of the variation of drag with yaw. However, using the data available from the tunnel tests of the same scale model, a variation of C_{D_f}, the fore drag coefficient, with α, the angle of attack, was obtained. The base drag increment was assumed constant for small angles of attack and the slope of $C_{D_{f_{\alpha^2}}}$ was used to obtain C_{D_0} and the corresponding K_{D_0} for the range data.

While five of the models had simple epicyclic yawing motion, the yawing motion of the remaining models was "tricyclic", which arises whenever aerodynamic asymmetries are present in the model. This type of motion is more difficult to handle. The theory is described in Ref. 3, and methods of analysis of this type of motion from spark range data are given in Refs. 6, 7, and 8. To obtain the lift force it was necessary to perform swerve reductions as described in Ref. 3 and 4.

The rolling motion of the warhead was studied on four of the models which had all vanes canted 2 degrees to the axis of symmetry to give counter clockwise rotation. The reduction procedure used can be found in Refs. 3, 6, 7, and 8. All of the models had two pins inserted in the base. One of these pins was sharp and one had a flat face. The range shadowgraphs could then be used at all stations to obtain a history of rolling motion throughout the range of photographic observations. On the four rounds with canted fins, yaw cards were used at the end of the range proper (approximately 1180 ft) to obtain further data points. $dC_\ell/d\frac{pb}{2V}$ or C_{ℓ_p} the rolling moment derivative due to rolling velocity and the rolling moment derivative due to canted surfaces $dC_\ell/d\delta$ or C_{ℓ_δ} were calculated where possible.

RESULTS

The resulting data from this program are listed in the form of coefficients in Table I, and plotted in graphical form versus Mach number in Appendix B. Wind Tunnel results (Ref. 1) are plotted where available. Table I shows the percentage error of fit as obtained from least square differential corrections and a notation as to the type of reduction used.

The variation of K_{D_0} and corresponding C_{D_0} with Mach number is shown in a graph, figure 10. The region near sonic velocity is covered, although only two models were fired in this region. Since the deceleration of these models was quite high, the timing data could be used in sections to determine more points then the usual mid-range average drag coefficient reduction. Table II lists transonic K_{D_0} and Mach numbers for these same rounds. In order to correct for yaw dependence of the drag coefficient it was assumed that the yaw drag coefficient $K_{D_{\delta 2}}$ was approximately the sonic value of the normal force coefficient. This is equivalent to assuming a zero value of the yaw-axial drag coefficient, $K_{DA_{\delta 2}}$. Since wind tunnel tests at Mach numbers 2.7 - 3.8 show that $K_{D_{\delta 2}} \doteq 3/4\ K_N$ and the magnitude of the entire yaw correction for these rounds is not more than three times the estimated accuracy of the data, the procedure seems to be justified. The total drag coefficient, C_{D_0} from wind tunnel data is plotted for comparison.

The ballistic moment coefficient K_M and corresponding C_{M_α} are plotted versus Mach number in figure 11. Since only a few models were assigned for firings near sonic velocity, the variation of the coefficient within this region could not be adequately determined in detail. The portion of the curve from $0.9 < M < 1.7$ is accordingly dashed rather than solid for K_M and other coefficients described hereafter. The shape used in fairing has been suggested by other firings of finned missiles for which the data were more complete in this velocity range. However data in this region should be used with some caution. The wind tunnel data are plotted in a graph for C_{M_α} and the agreement is believed to be within the accuracy of the data.

Figures 12 and 13 show the ballistic lift coefficient K_L and a C_{L_α} scale and the ballistic normal force coefficient, K_N, with corresponding, C_{N_α}, respectively. Wind tunnel results for C_{N_α} are plotted and again show good agreement.

Figure 14 shows the damping moment coefficient, K_H, and the corresponding $(C_{M_q} + C_{M_{\dot\alpha}})$ plotted versus Mach number. Round 2873 demonstrated a motion which caused some difficulty in the reduction of data. The coefficients for this round, and especially K_H, are not well determined. It may be noted in the tabulation of data for 2873 that the damping of both of the arms of motion are assumed equal although actually the precessional arm was the only one adequately determined.

An average of the damping of the nutational and precessional arms of the motion is shown as $\frac{\lambda_1 + \lambda_2}{2}$ versus Mach number in figure 15. The reason for plotting an average value of damping is that finned projectiles deviate often from the theoretical equality of the damping arms. This deviation is usually a result of asymmetries. An average damping is considered somewhat more representative.

The roll derivatives C_{l_p} and C_{l_δ} were determined at three velocities and are plotted versus Mach numbers in figures 16 and 17. Both rounds, at approximately Mach number 2.0 struck some obstruction at the end of the range and the extension of the roll data through use of yaw cards was impossible. This point therefore is subject to some doubt. Theoretical calculations were made using reference 6 and these curves are plotted in figures 16 and 17. The wind tunnel results for C_{l_δ} were reduced to the same coefficient base as in reference 6 and are shown. Data of finned rolling missiles, reference 6, and unpublished data of this laboratory would indicate a good agreement with theory for $M \geq 1.7$ and the shape assumed in the fairing for $1 \leq M \leq 1.7$.

REMARKS

It should be noted that this program, as originally scheduled, required no coverage of the sonic region and therefore the use of four of the models to indicate a direction into this rather critical region, did not permit an adequate study of the more sensitive parameters, but did at least indicate magnitudes of the numbers to be expected.

The author is indebted to Pfc. Bernard Hull* of the Free Flight Branch, for aid in some of the analysis of data and compilation of results and to Leonard C. MacAllister, also of the Free Flight Branch, for many suggestions throughout the program and aid in the analysis of the data.

Walter K. Rogers

WALTER K. ROGERS, JR.

* Formerly an engineer with David Taylor Model Basin

REFERENCES

1. Krieger, R. H., and Hughes, J. M., Wind Tunnel Tests of the Redstone Arsenal Missile, "Redstone" XSSM-A-14 Warhead Model, BRL Memorandum Report 671 (1953).

2. Rogers, W. K., The Transonic Free Flight Range, BRL Report 849 (1953).

3. Murphy, C. H., Data Reduction for the Free Flight Spark Ranges, BRL Report 900 (1954).

4. Schmidt, L. E., Aerodynamic Coefficients Determined from the Swerve Reduction, BRL Memorandum Report 599 (1952).

5. MacAllister, L. C., On the Use of Plastic Sabots for Free Flight Testing, BRL Memorandum Report 782 (1954).

6. Bolz, R. E., and Nicolaides, J. D., A Method of Determining Some Aerodynamic Coefficients from Supersonic Free Flight Tests of a Rolling Missile, BRL Report 711 (1949).

7. Nicolaides, J. D., On the Free Flight Motion of Missiles Having Slight Configurational Asymmetries, BRL Report 858 (1953).

8. MacAllister, L. C., Comments on the Preliminary Reduction of Symmetric and Asymmetric Yawing Motions of Free Flight Range Models, BRL Memorandum Report 781 (1954).

REDSTONE WARHEAD

DATA TABULATION - TABLE I

Range Rd No	Mach No (mid range)	$\bar{\delta}^2$	K_D	ϵK_D %	K_{D_0}	C_{D_0}	Damping λ_1 1/ft	Damping λ_2 1/ft	Rates b_1 °/ft	Rates b_2 °/ft	k_1 rad	k_2 rad	k_3 rad	K_M	ϵK_M %	C_{M_α} 1/deg	K_L
2873	1.009	10.78	*	*	*	*	.00102	**	-2.03	2.03 +	055	002	.002	-.530	0.8	-.024	1.18
2877	1.020	8.40	*	*	*	*	.00183	.00173	-1.89	1.88	032	032	.003	-.464	0.7	-.021	1.13
2876	1.373	25.65	.2458	.21	.237	.604	.00212	.00146	-1.69	1.46	052	066		-.319	0.5	-.014	1.17
2874	1.463	8.38	.2276	.05	.225	.573	.00201	.00200	-1.52	1.52	024	038	005	-.298	0.5	-.013	1.29
2358	1.820	34.55	.2129	.14	.201	.511	.00177	.00163	-1.67	1.65	078	058		-.352	0.6	-.016	1.23
2360	1.910	5.91	.1964	.10	.195	.495	.00174	.00169	-1.62	1.57	022	031		-.323	0.6	-.014	1.15
2316	1.954	12.41	.1935	.16	.189	.481	.00183	.00182	-1.60	1.59	037	043		-.322	0.5	-.014	1.32
2452	2.020	22.95	.1902	.81	.183	.465	.00274	.00081	-1.73	1.52	039	070		-.336	1.1	-.015	1.32
2451	2.033	8.78	.1851	.11	.182	.463	Trajectory very High							--	--	--	--
2314	2.500	5.27	.1579	.09	.156	.397	.00152	.00153	-1.45	1.45 +	026	026		-.279	0.8	-.012	1.17
2359	2.511	9.46	.1595	.03	.156	.397	.00155	.00155	-1.52	1.52 +	036	027	003	-.291	2.3	-.013	1.31
2442	2.943	1.58	.1384	.11	.138	.351	.00136	.00120	-1.43	1.40	012	018		-.252	1.0	-.011	1.26
2443	2.951	1.80	.1369	.08	.136	.346	Small Amount of Data							--	--	--	--
2445	3.137	2.59	.1310	.11	.130	.331	.00109	.00109	-1.39	1.39 +	016	024	006	-.244	1.0	-.011	1.11
2444	3.177	11.97	.1356	.51	.132	.336	.00141	.00141	-1.40	1.40 +	034	045	014	-.248	3.5	-.011	1.21

* See Table II

** K_2 too small, λ_2 was assumed equal to λ_1

\+ Yaw reduction required that $b_1 = -b_2$

REDSTONE WARHEAD

DATA TABULATION - TABLE I (cont)

Range Rd No	S_L Ft.	ϵK_L %	K_N	C_{N_α}	K_H	ϵK_H %	$C_{M_q} + C_{M_\alpha}$	C_{ℓ_p}	$C_{\ell_{\delta_v}}$	Type of Data Reduction
2873	04	0.19	1.44	-.064	2.30	7.4	-.204	1.15	1.43	TY & S with R
2877	.04	11.4	1.39	-.062	5.01	8.0	-.445	--	--	TY & S
2876	.11	6.9	1.42	-.063	4.90	5.3	-.436	0.52	1.19	EY & S + R
2874	.07	5.7	1.52	-.068	5.40	6.0	-.480	--	--	TY & S with R
2358	.11	4.9	1.45	-.064	4.38	5.5	-.389	--	--	EY & S
2360	.05	5.9	1.35	-.060	4.50	5.4	-.400	--	--	EY & S
2316	.08	4.9	1.51	-.067	4.67	3.9	-.415	--	--	EY & S
2452	.11	4.2	1.51	-.067	4.52	8.6	-.402	0.62	1.12	EY & S + R
2451	--	--	--	--	--	--	--	--	--	---
2314	.05	12.4	1.33	-.059	3.74	7.9	-.332	--	--	EY & S
2359	.04	7.9	1.47	-.065	3.69	8.4	-.328	--	--	TY & S
2442	.04	5.4	1.40	-.062	2.83	14.8	-.252	--	--	EY & S
2443	--	--	--	--	--	--	--	--	--	---
2445	.04	4.9	1.24	-.055	2.39	28.2	-.212	--	--	TY & S
2444	.05	3.0	1.35	-.060	3.29	--	-.292	--	--	TY & S

Conversion Formula

$K_D = \frac{\pi}{8} C_D$

$K_L = \frac{-\pi}{8} C_{L_\alpha} \times 57.3$

$K_N = \frac{-\pi}{8} C_{N_\alpha} \times 57.3$

$K_M = \frac{\pi}{8} C_{M_\alpha} \times 57.3$

$K_H = \frac{-\pi}{16} (C_{M_q} + C_{M_{\dot\alpha}}) \times 57.3$

$R_e = \frac{\rho V \ell}{\mu}$

where ℓ is body length

$= 4.341 \times d$

For this program

$\frac{R_e}{M} = .758 \times 10^7$

Type of Data Reduction
- TY - Tricycle Yaw
- EY - Epicycle Yaw
- S - Swerve
- R - Roll

TABLE II

TRANSONIC ROUNDS

Round No. 2873

Mach No.	$\bar{\delta}^2$	K_D	K_{D_0}
1.037	34.47	.267	.252
1.024	27.90	.264	.252
1.009	22.32	.259	.249
1.003	19.70	.257	.248
.978	12.15	.220	.215
.971	10.83	.206	.201

Note: 10 timing stations

Round No. 2877

Mach No.	$\bar{\delta}^2$	K_D	K_{D_0}
1.066	14.11	.276	.270
1.052	11.68	.269	.264
1.046	10.83	.269	.264
1.039	8.86	.269	.264
1.022	7.22	.263	.260
1.016	6.07	.260	.258
.997	4.13	.246	.245
.991	3.81	.239	.238
.989	3.49	.234	.232
.979	2.89	.218	.217

Note: 14 timing stations

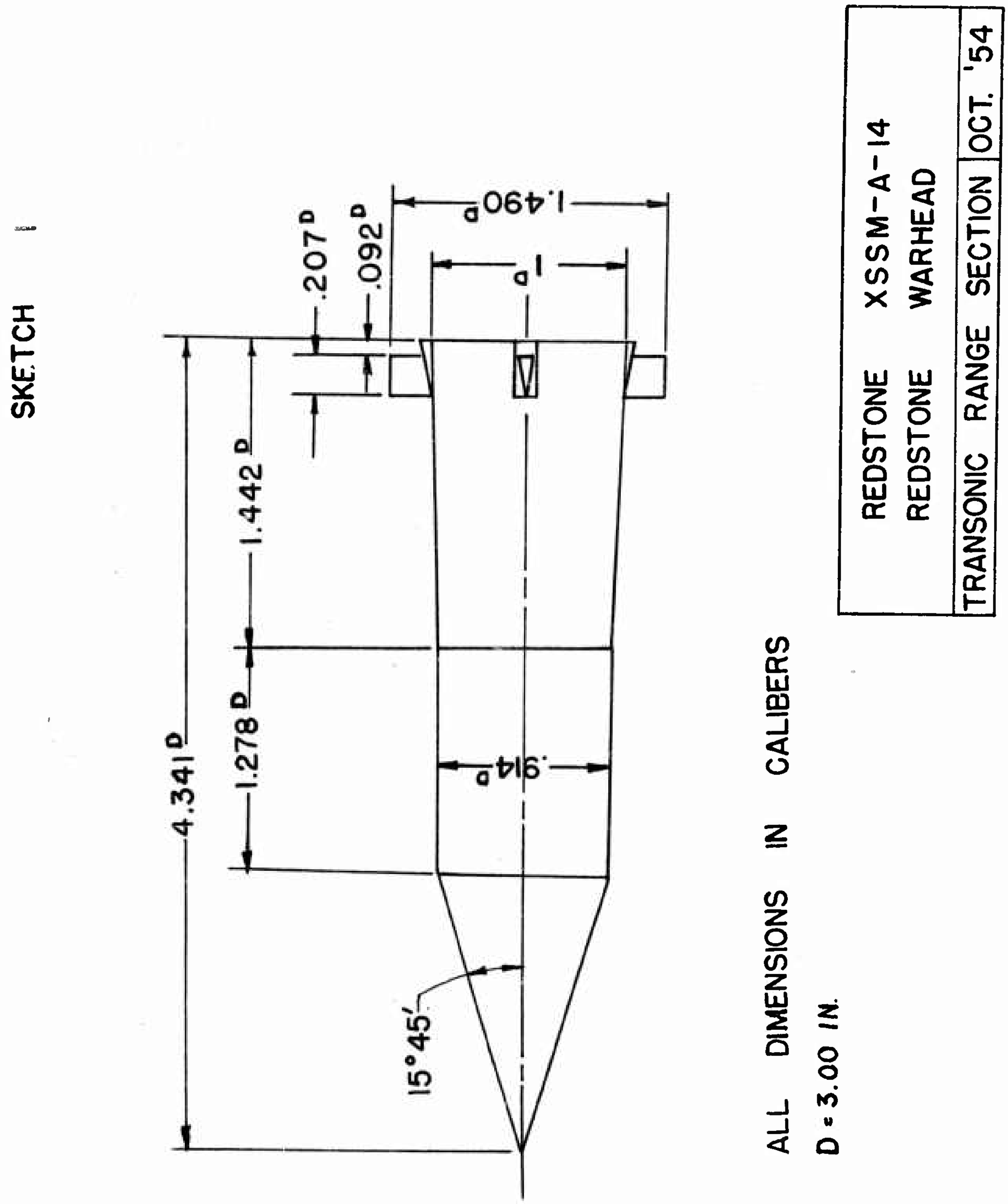

SKETCH
1.490 D
1 D
.207 D
.092 D
1.442 D
1.278 D
4.341 D
.914 D
15°45'
ALL DIMENSIONS IN CALIBERS
D = 3.00 IN.
REDSTONE XSSM-A-14
REDSTONE WARHEAD
TRANSONIC RANGE SECTION
OCT. '54

SKETCH 2

MODEL IN PLASTIC SABOT

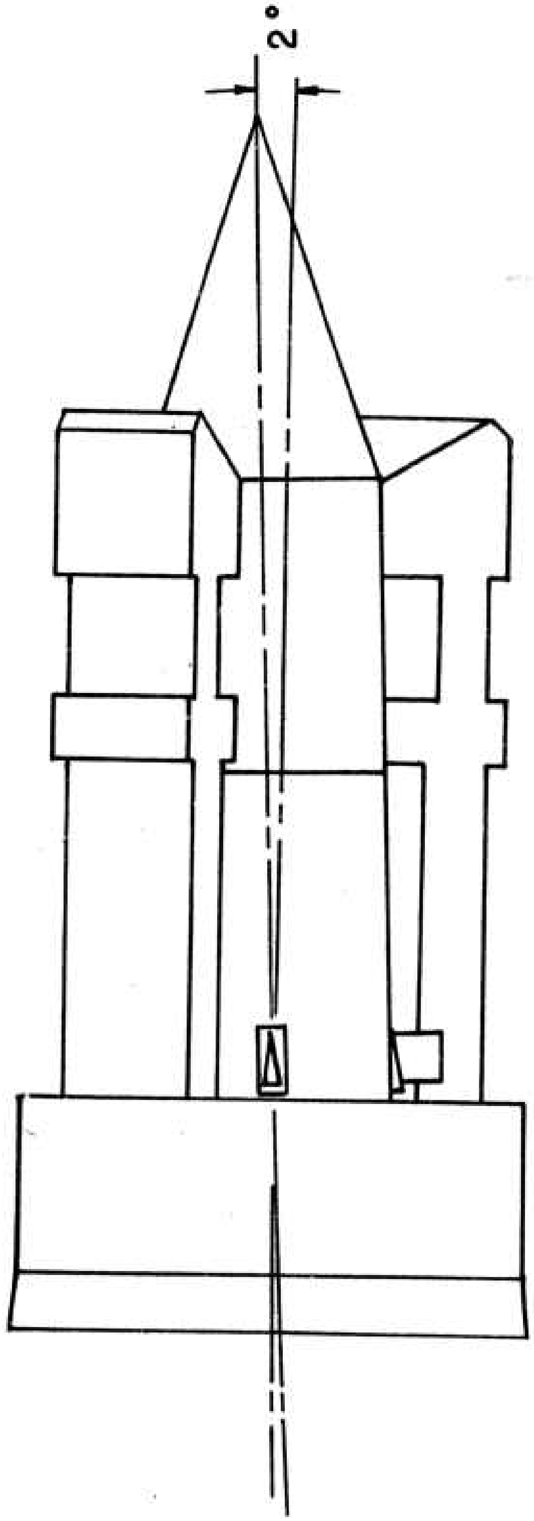

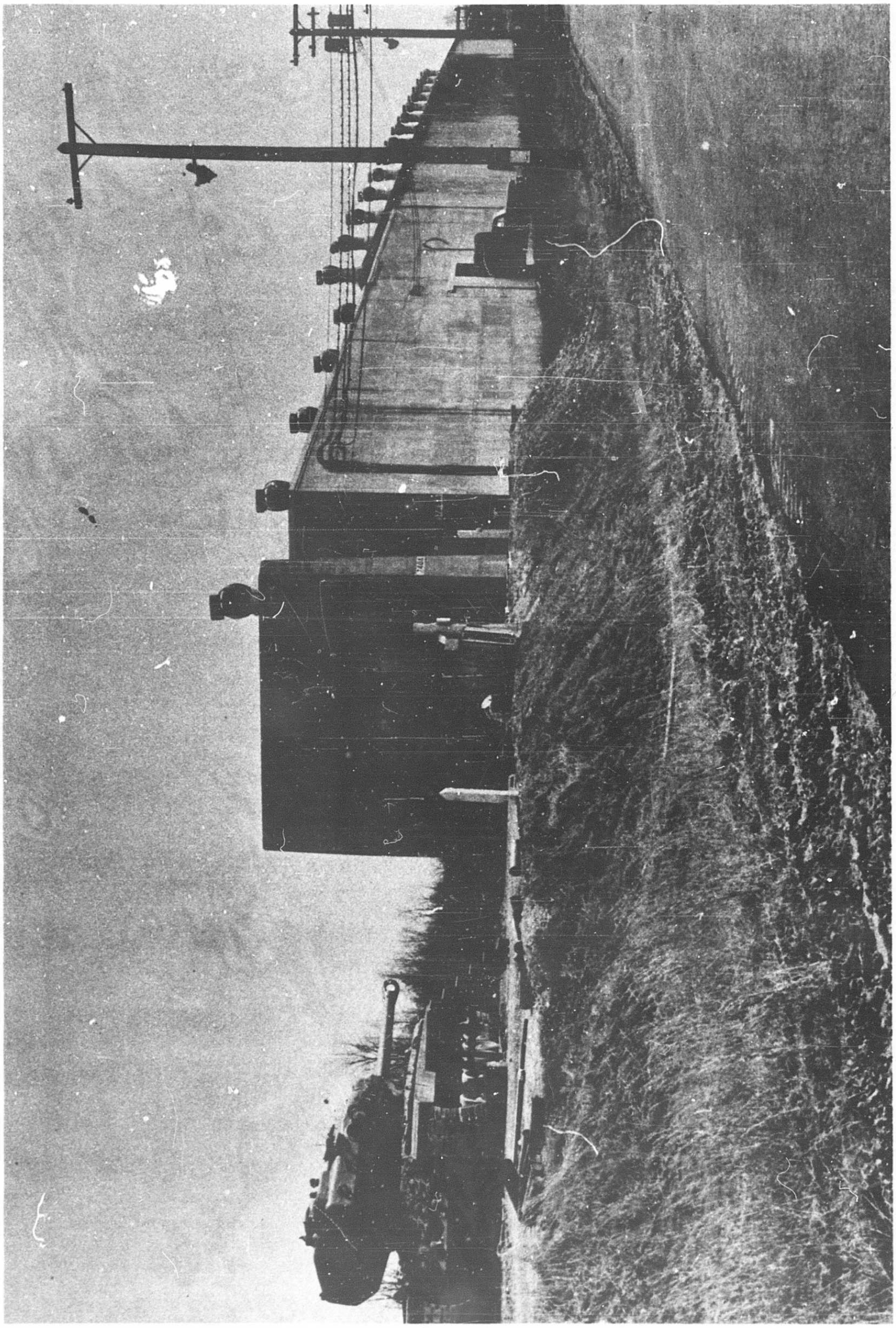

Figure 1. Exterior of Range. View Downrange From Firing Ramp.

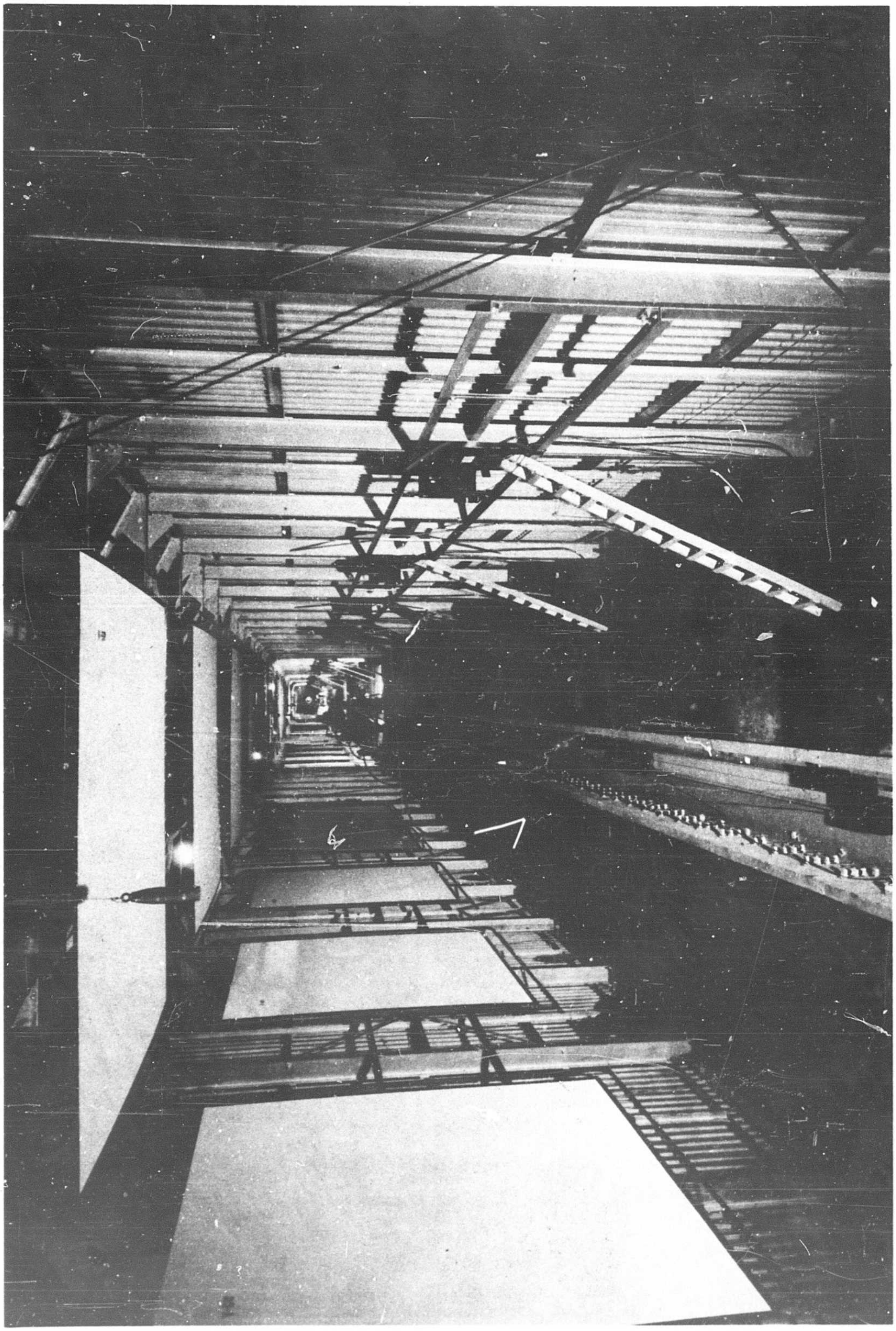

Figure 2. Interior of Transonic Free Flight Range.

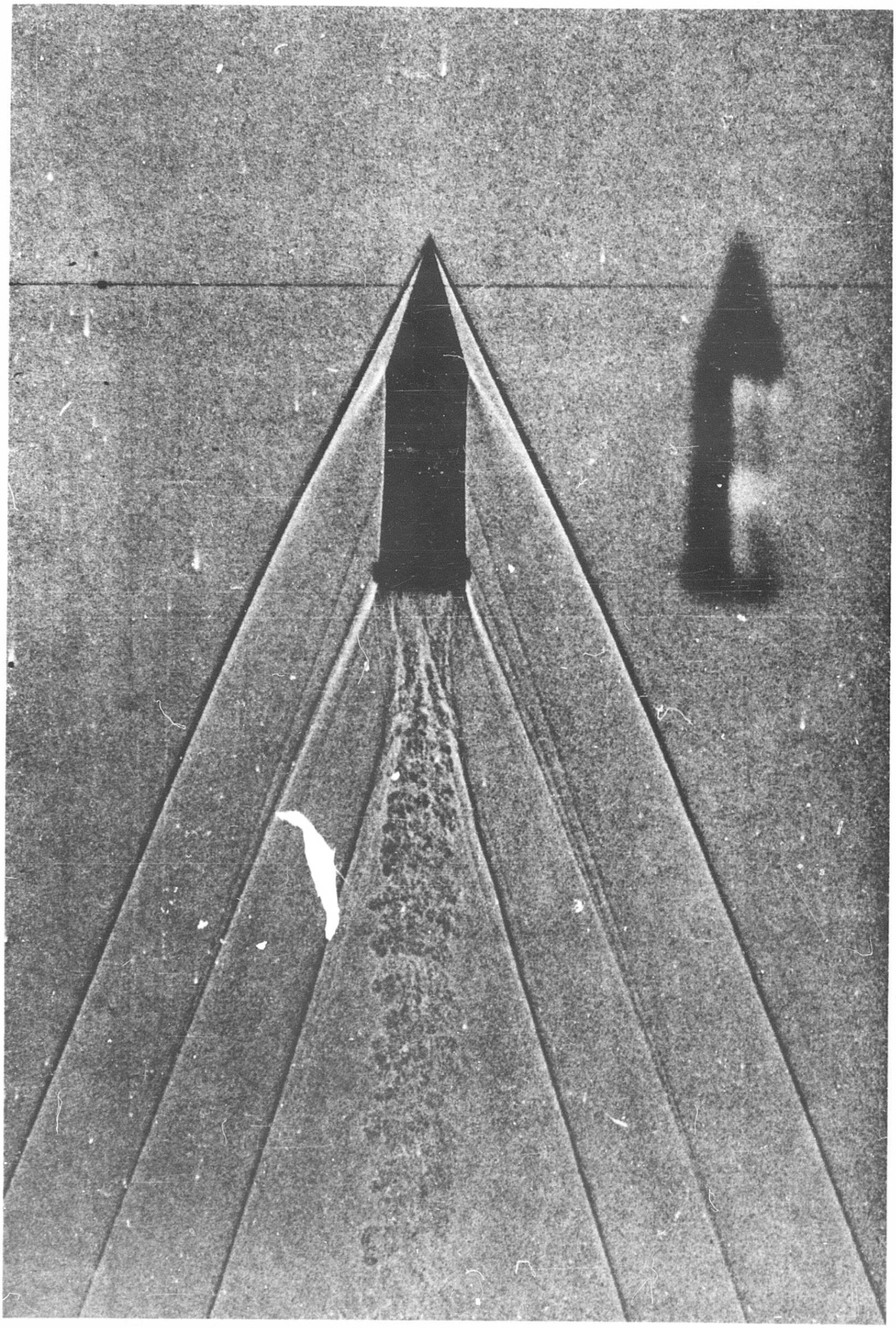

Figure 3. Round No. 2444 in Shadowgraph
Velocity: Approx. 3580 ft/sec
Mach No: Approx. 3.18

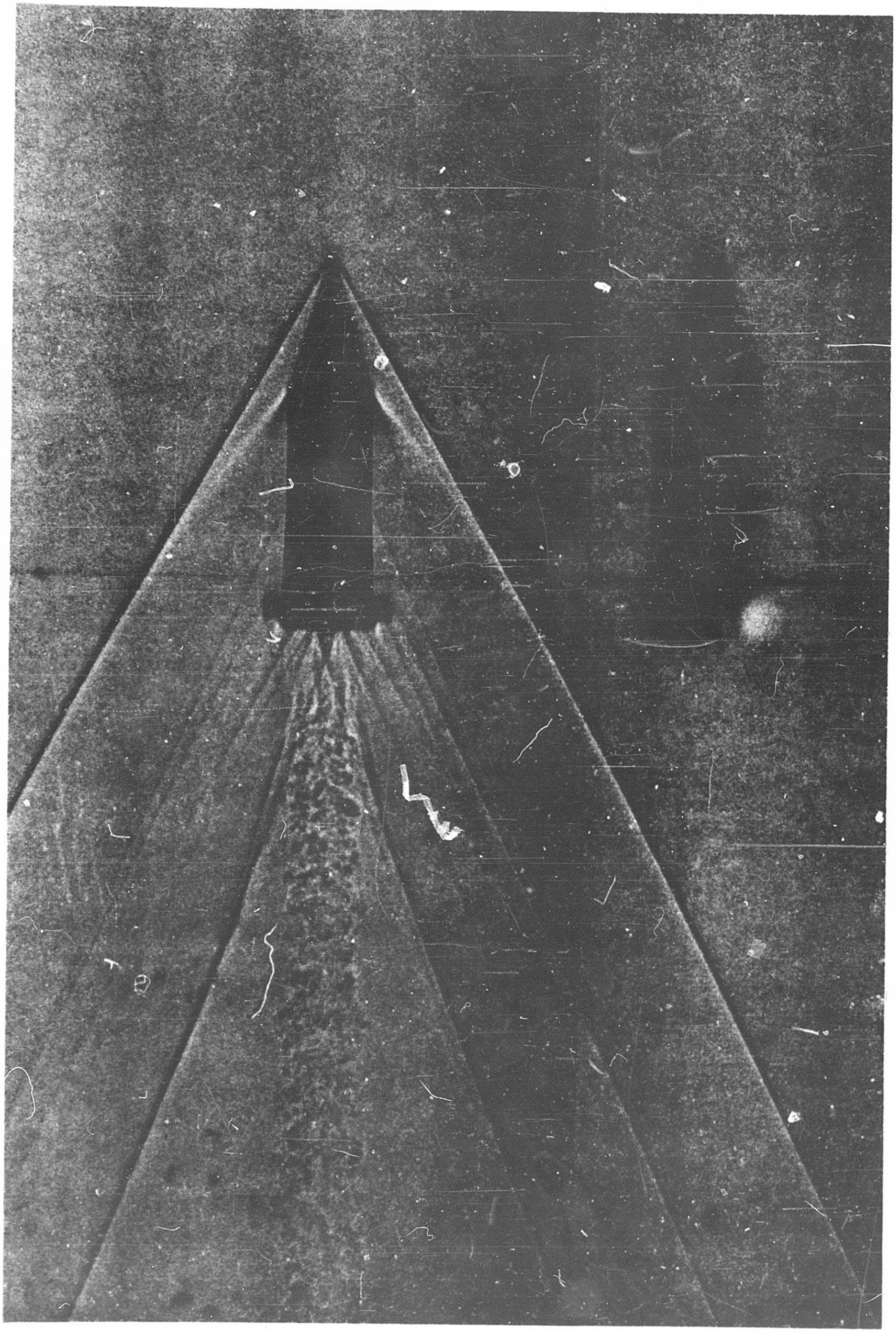

Figure 4. Round No. 2314 in Shadowgraph
Velocity: Approx. 2820 ft/sec.

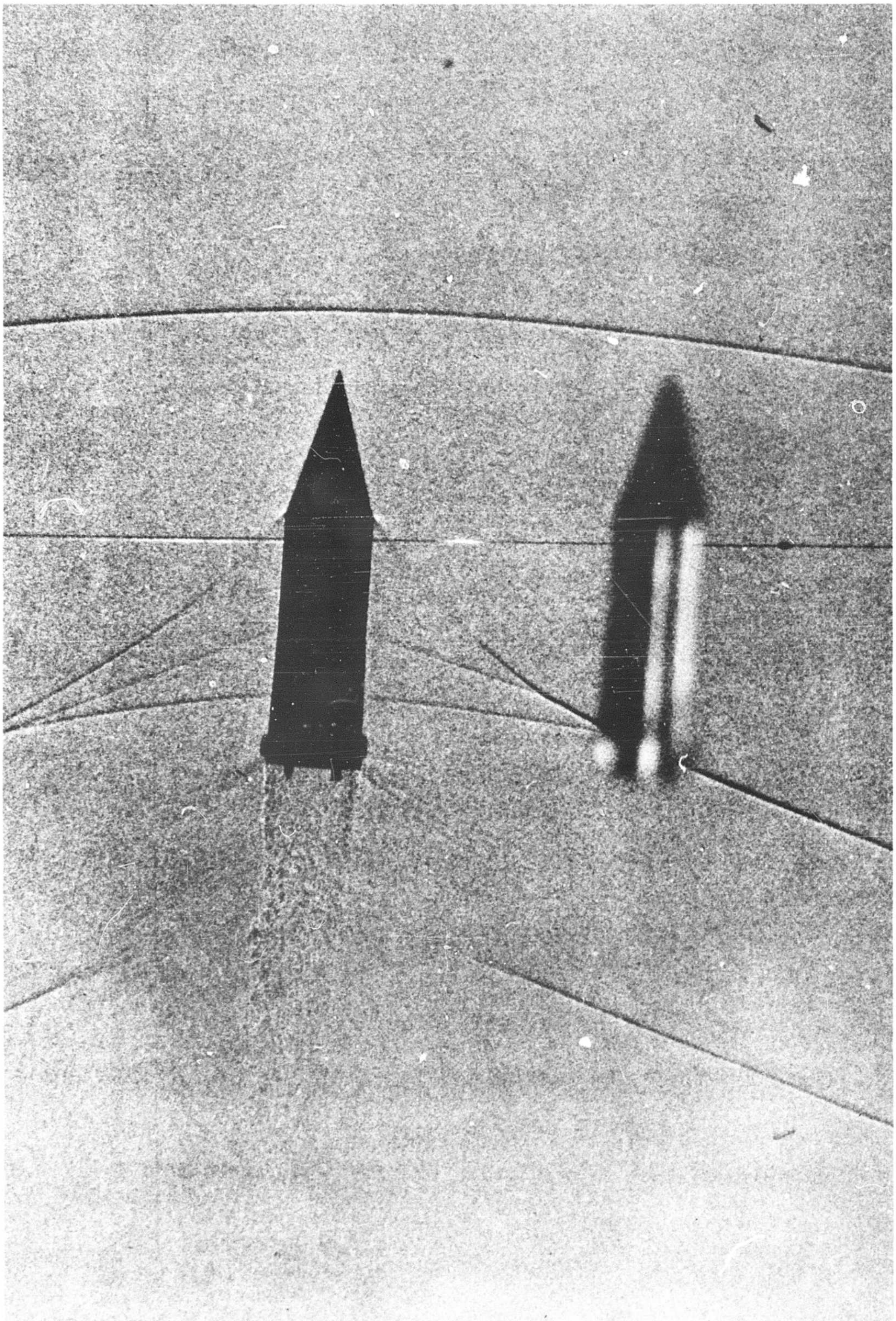

Figure 5. Round No. 2873 in Shadowgraph
Velocity: Approx. 1178 ft/sec.
Mach No: Approx. 1.04

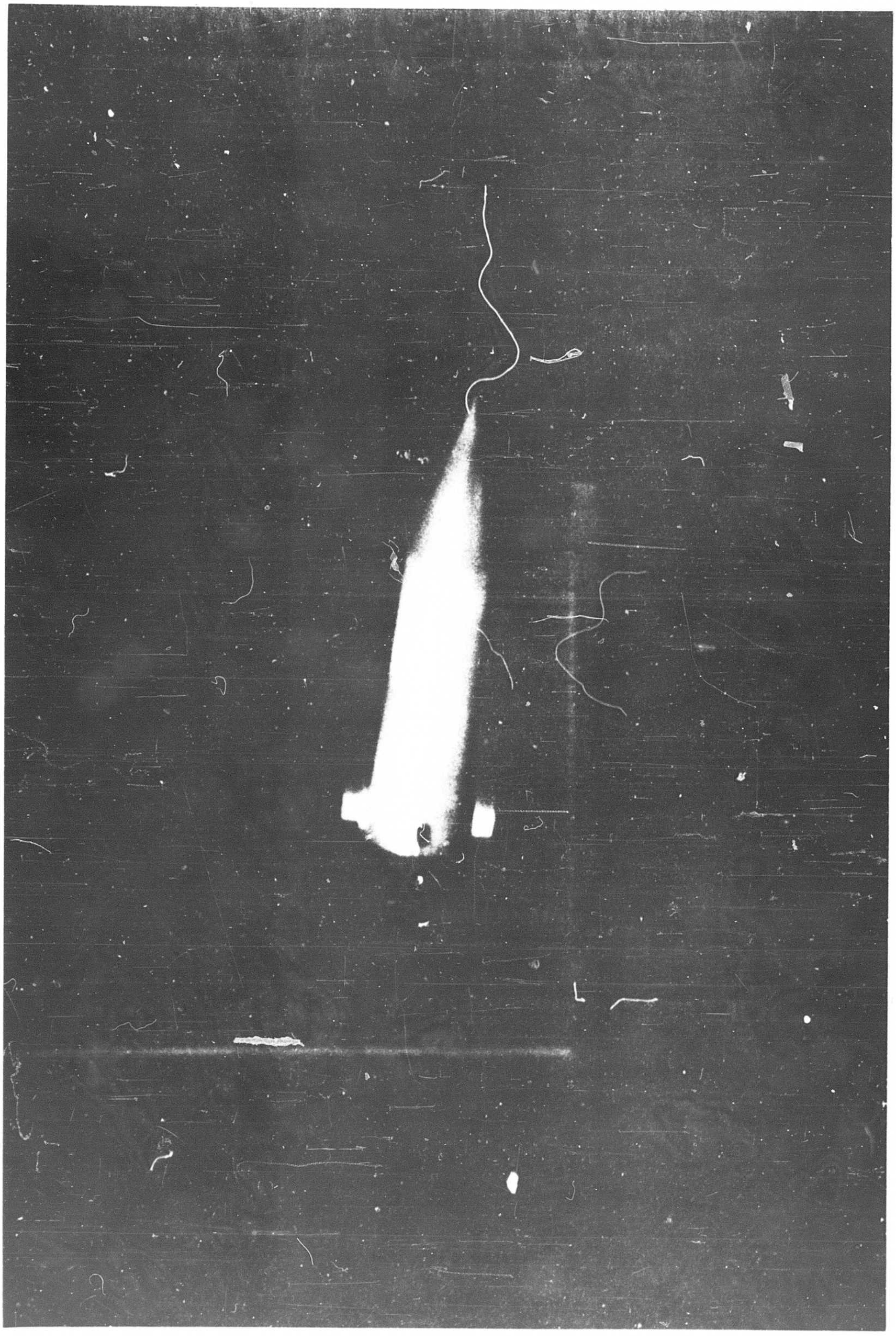

Figure 6. Round No. 2358 in Microflash (Direct Photograph)
Velocity: Approx. 2050 ft/sec
Mach No: Approx. 1.82

Figure 7. Motion Pictures of Launching of Round No. 2876
Camera: 16mm (1/2 frame) Fastax.
Lens: Listed by Each Print.
Speed: Approx. 12,000 Frames per Second.

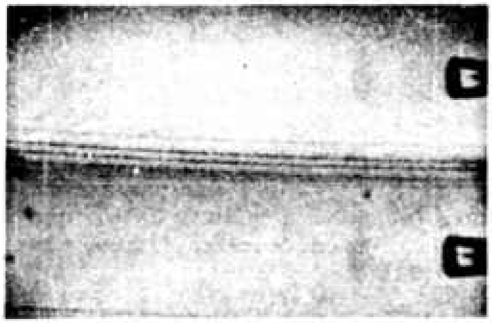

7a. Nose of Model Just Appearing Within the Muzzle Brake of the Gun. The Absence of Gases Indicates Good Obturation. (35mm Lens)

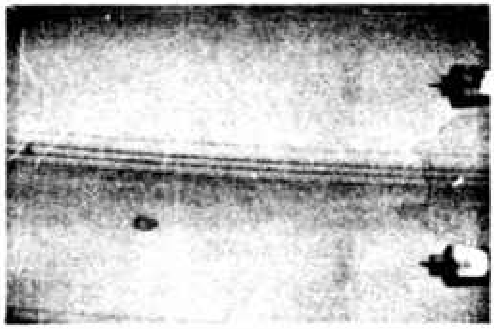

7b. Flame and Gases Just Appearing Within the Muzzle Brake. (35mm Lens)

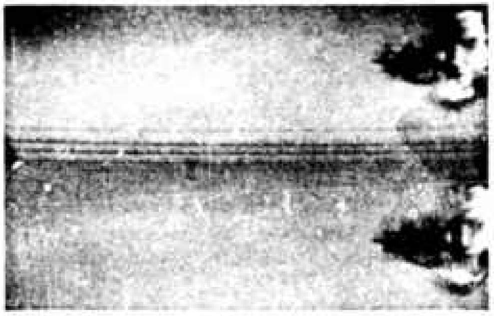

7c. Sabot and Model Clear of Gun. (35mm Lens)

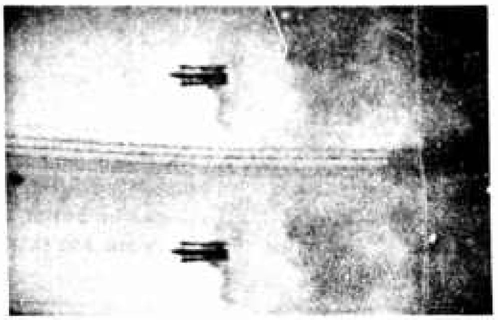

7d. Sabot and Model Flying Free Ahead of Gas Envelope. (35mm Lens)

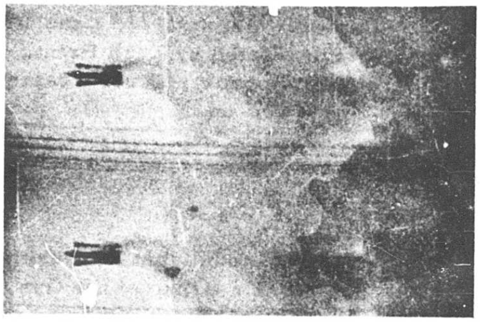

Figure 7e. Sabot Begins to Open, Approx. 8 ft. From Muzzle. (35mm Lens)

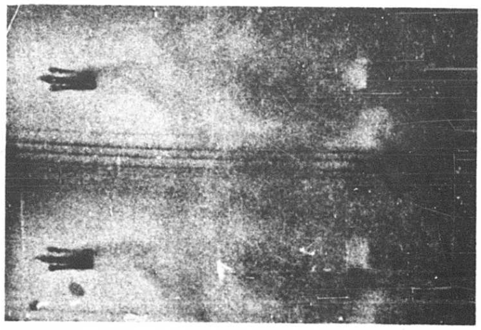

7f. Model Just Beginning to Move Out of Sabot, Approx. 9 ft. From the Muzzle. (35mm Lens)

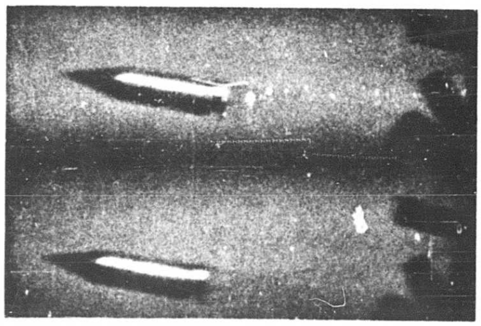

7g. Model Flying Free With Sabot Parts Following Approx. 1 ft. Behind. This Occurred at About 50 ft. From The Muzzle. (6" Lens)

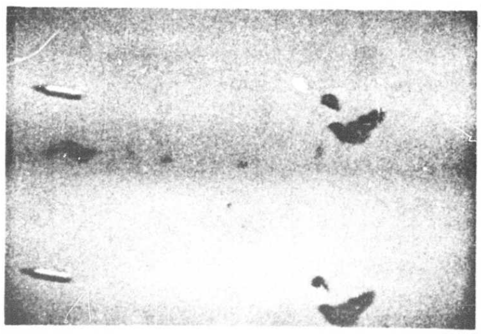

7h. Model Well Ahead of Sabot Parts at Approx. 90 ft. from Muzzle (2" Lens)

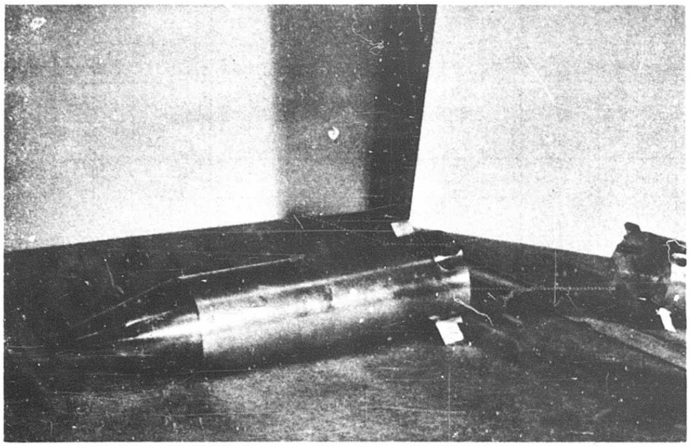

Figure

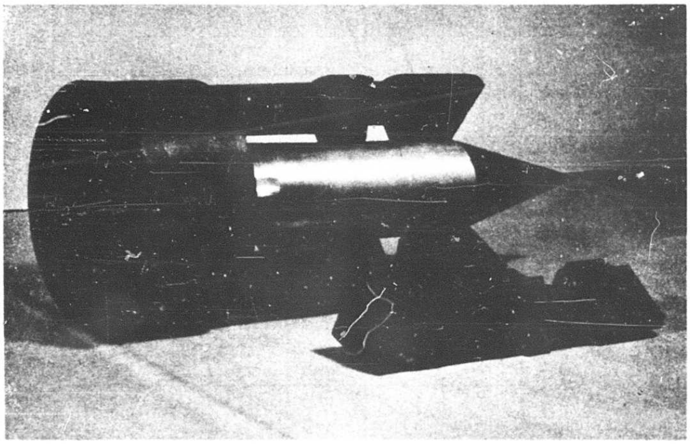

Figur

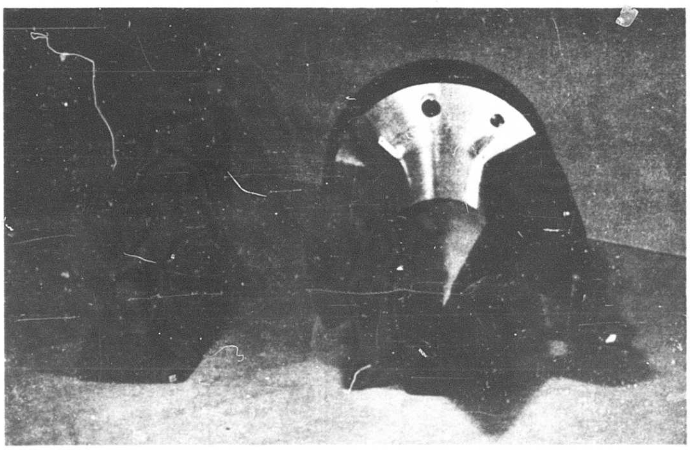

Figur

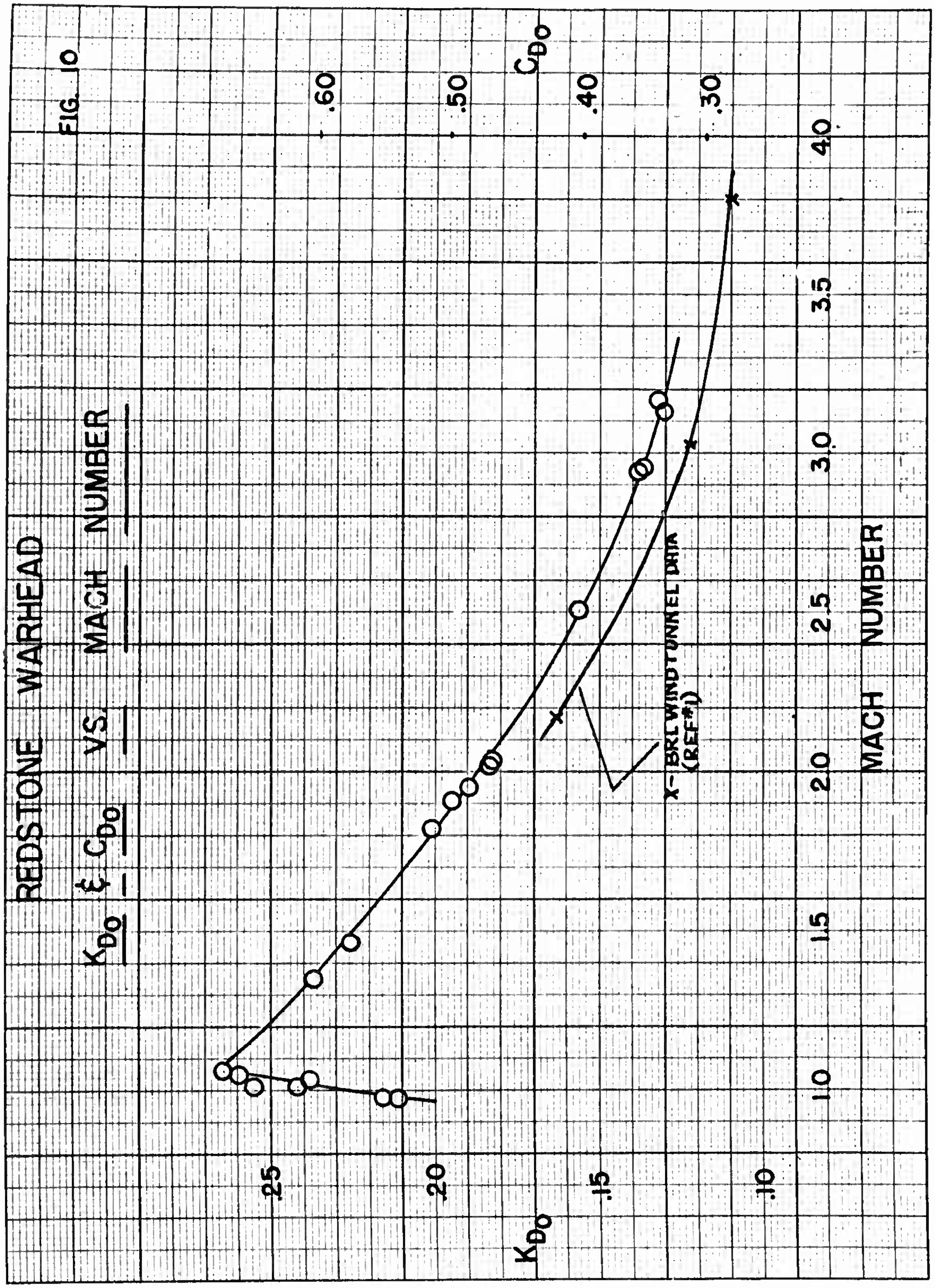
FIG. 10
REDSTONE WARHEAD
K_{DO} & C_{DO} VS MACH NUMBER
C_{DO}
.60
.50
.40
.30
K_{DO}
.25
.20
.15
.10
1.0
1.5
2.0
2.5
3.0
3.5
4.0
MACH NUMBER
X-BRL WINDTUNNEL DATA (REF #1)

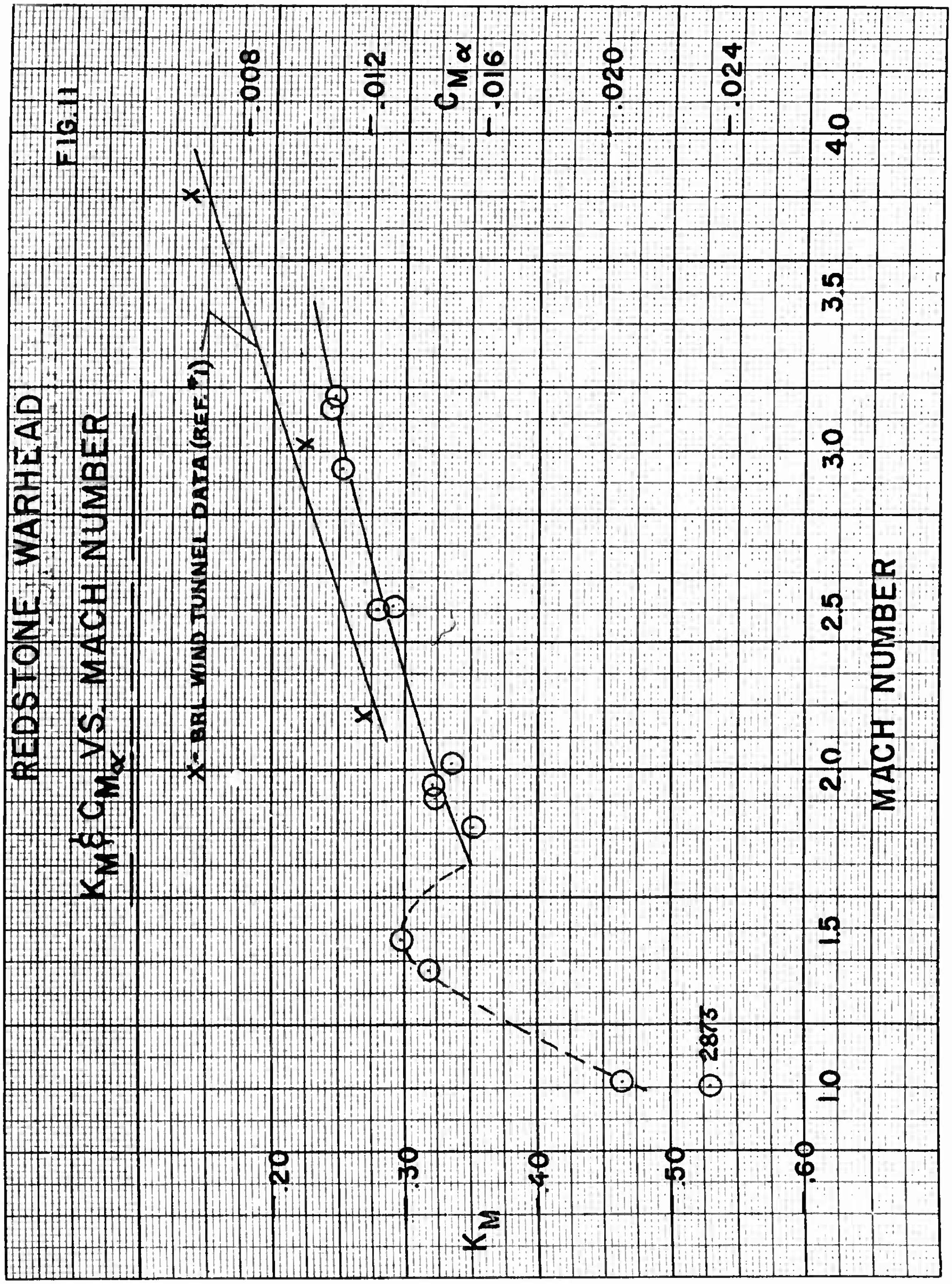
FIG. 11
REDSTONE WARHEAD
K_M & $C_{M\alpha}$ VS. MACH NUMBER
X - BRL WIND TUNNEL DATA (REF. #1)
.008
.012
$C_{M\alpha}$
.016
.020
.024
2873
.20
.30
.40
.50
.60
K_M
1.0
1.5
2.0
2.5
3.0
3.5
4.0
MACH NUMBER

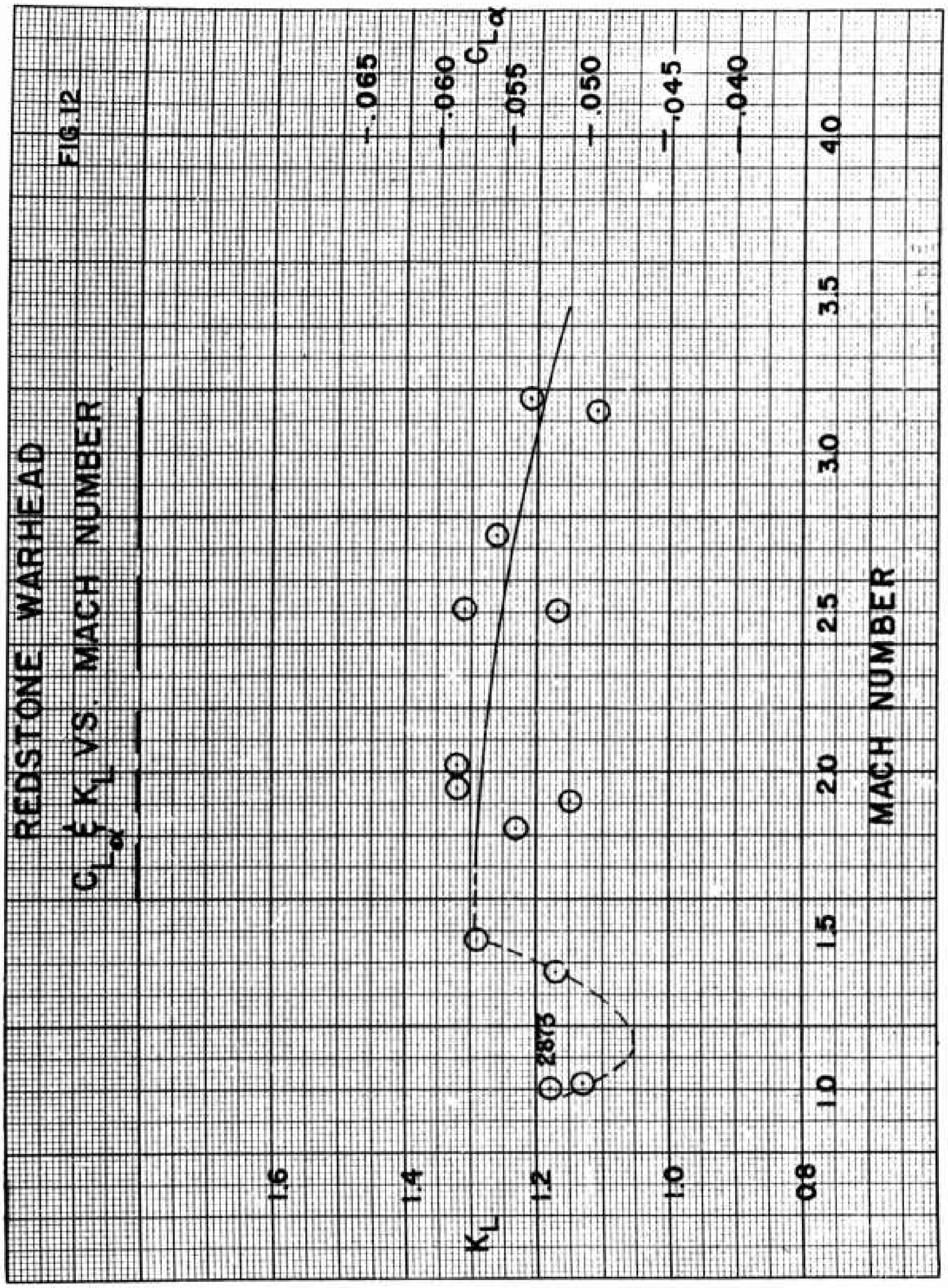
FIG. 12
REDSTONE WARHEAD
C_{L_α} & K_L VS. MACH NUMBER
C_{L_α}
.065
.060
.055
.050
.045
.040
K_L
1.6
1.4
1.2
1.0
0.8
2875
1.0
1.5
2.0
2.5
3.0
3.5
4.0
MACH NUMBER

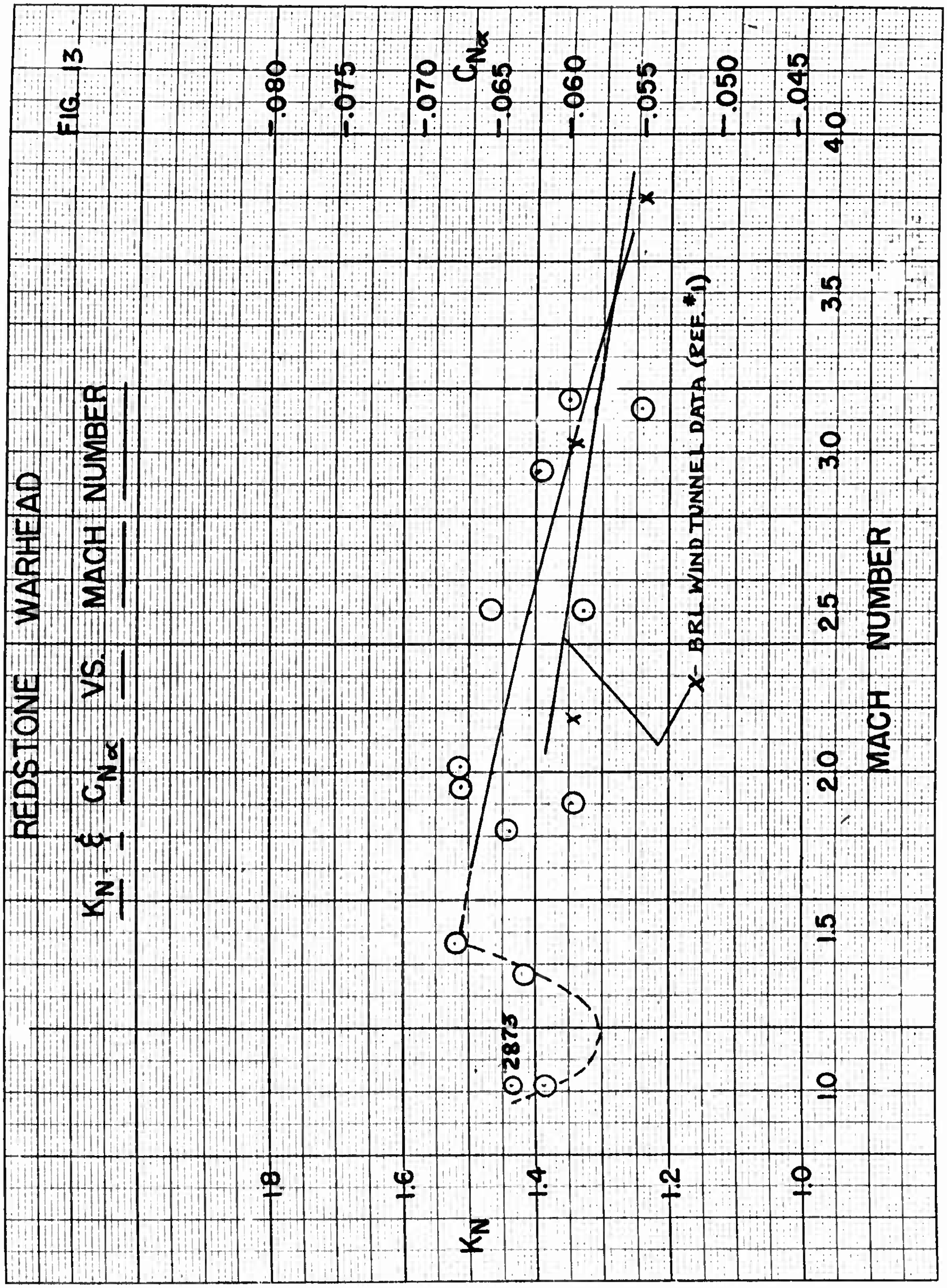
FIG. 13
REDSTONE WARHEAD
K_N & C_Nα VS. MACH NUMBER
C_Nα
-.080
-.075
-.070
-.065
-.060
-.055
-.050
-.045
K_N
1.8
1.6
1.4
1.2
1.0
MACH NUMBER
1.0
1.5
2.0
2.5
3.0
3.5
4.0
2873
X- BRL WIND TUNNEL DATA (REF #1)

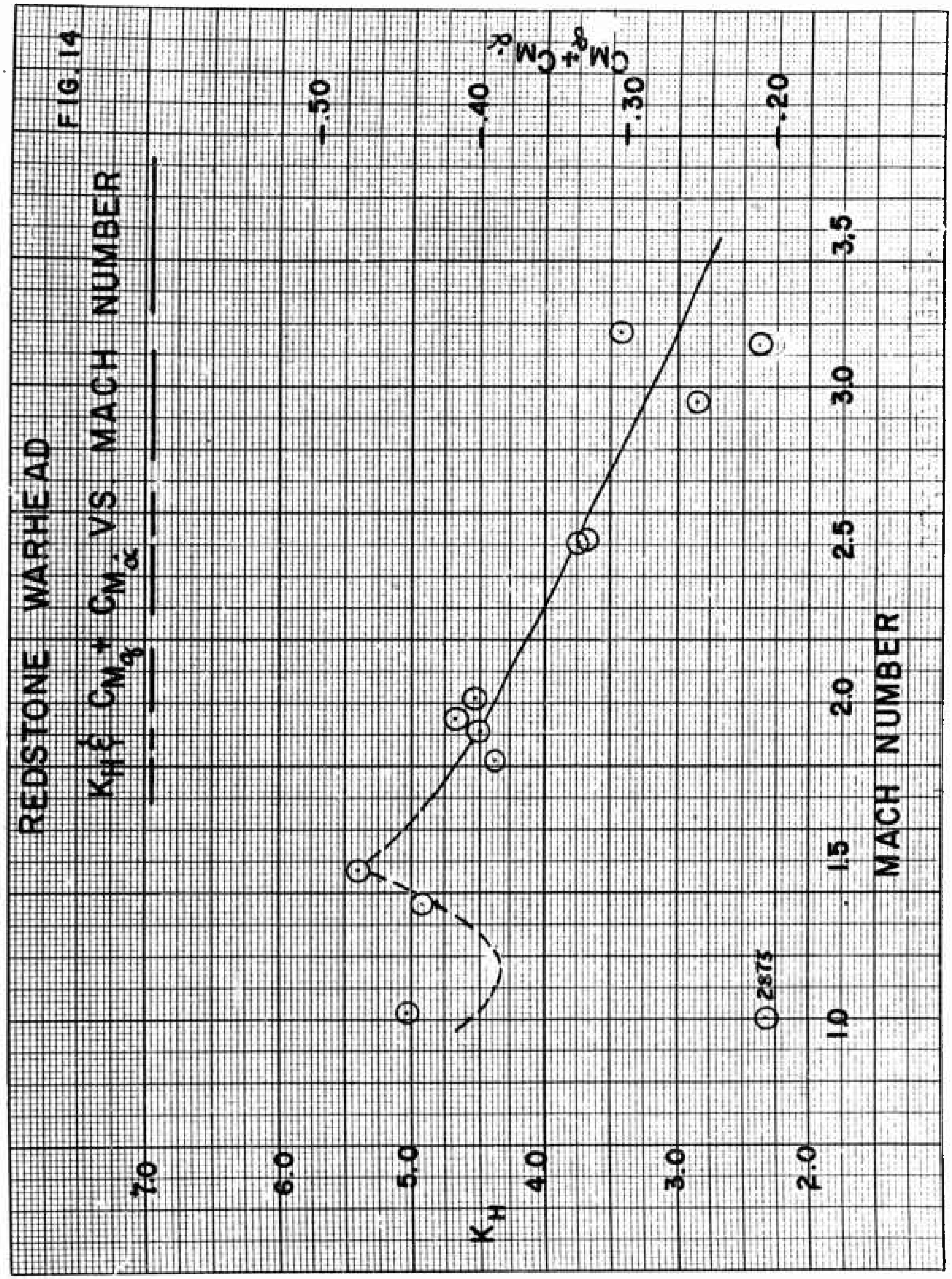
FIG. 14
REDSTONE WARHEAD
K_H & $C_{M_q} + C_{M_{\dot\alpha}}$ VS. MACH NUMBER
$C_{M_q} + C_{M_{\dot\alpha}}$
-.50
-.40
-.30
-.20
K_H
7.0
6.0
5.0
4.0
3.0
2.0
MACH NUMBER
1.0
1.5
2.0
2.5
3.0
3.5
2875

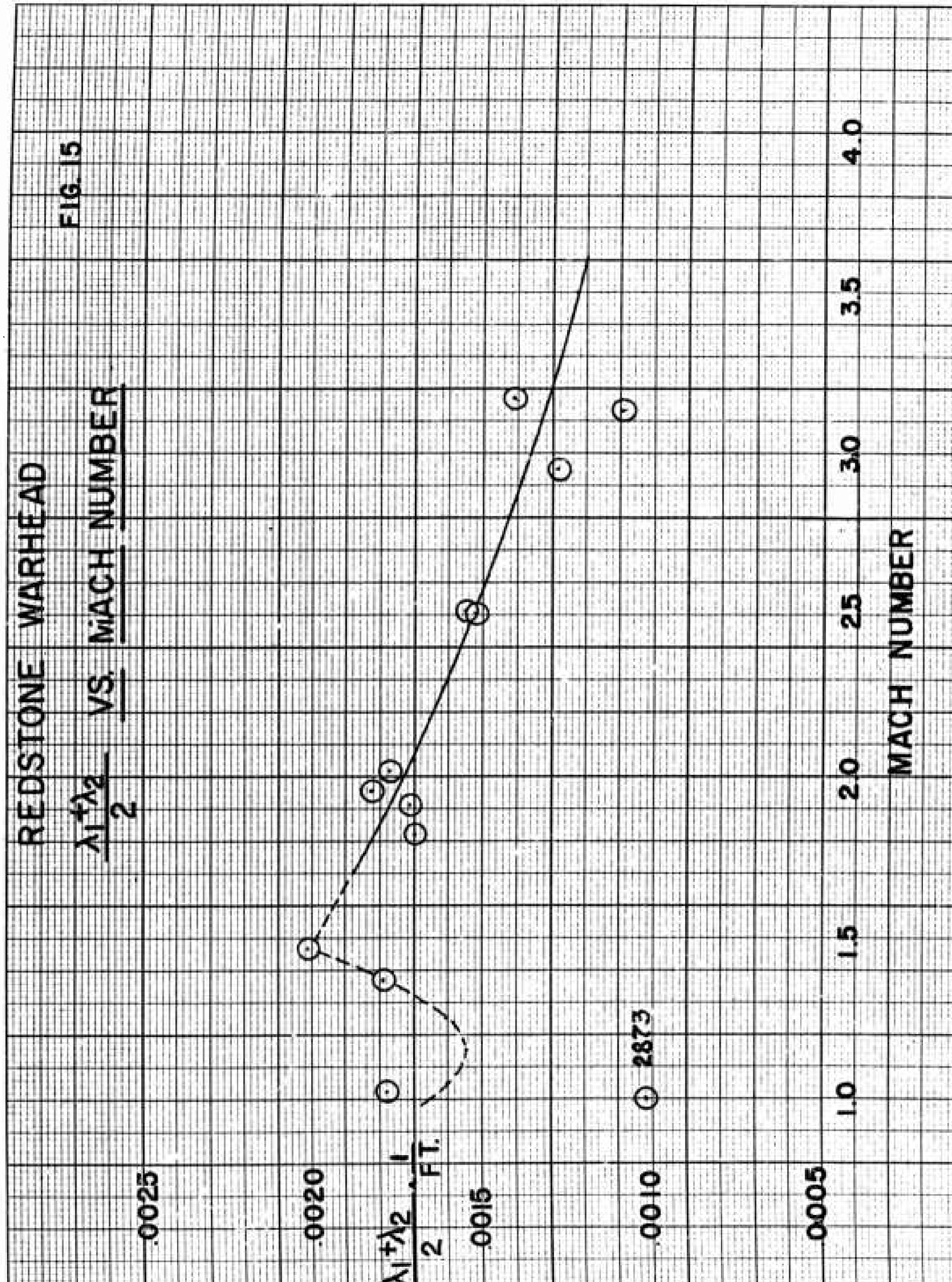
REDSTONE WARHEAD
$\frac{\lambda_1+\lambda_2}{2}$ VS. MACH NUMBER
FIG. 15
$\frac{\lambda_1+\lambda_2}{2}$, $\frac{1}{FT.}$
.0025
.0020
.0015
.0010
.0005
2873
1.0
1.5
2.0
2.5
3.0
3.5
4.0
MACH NUMBER

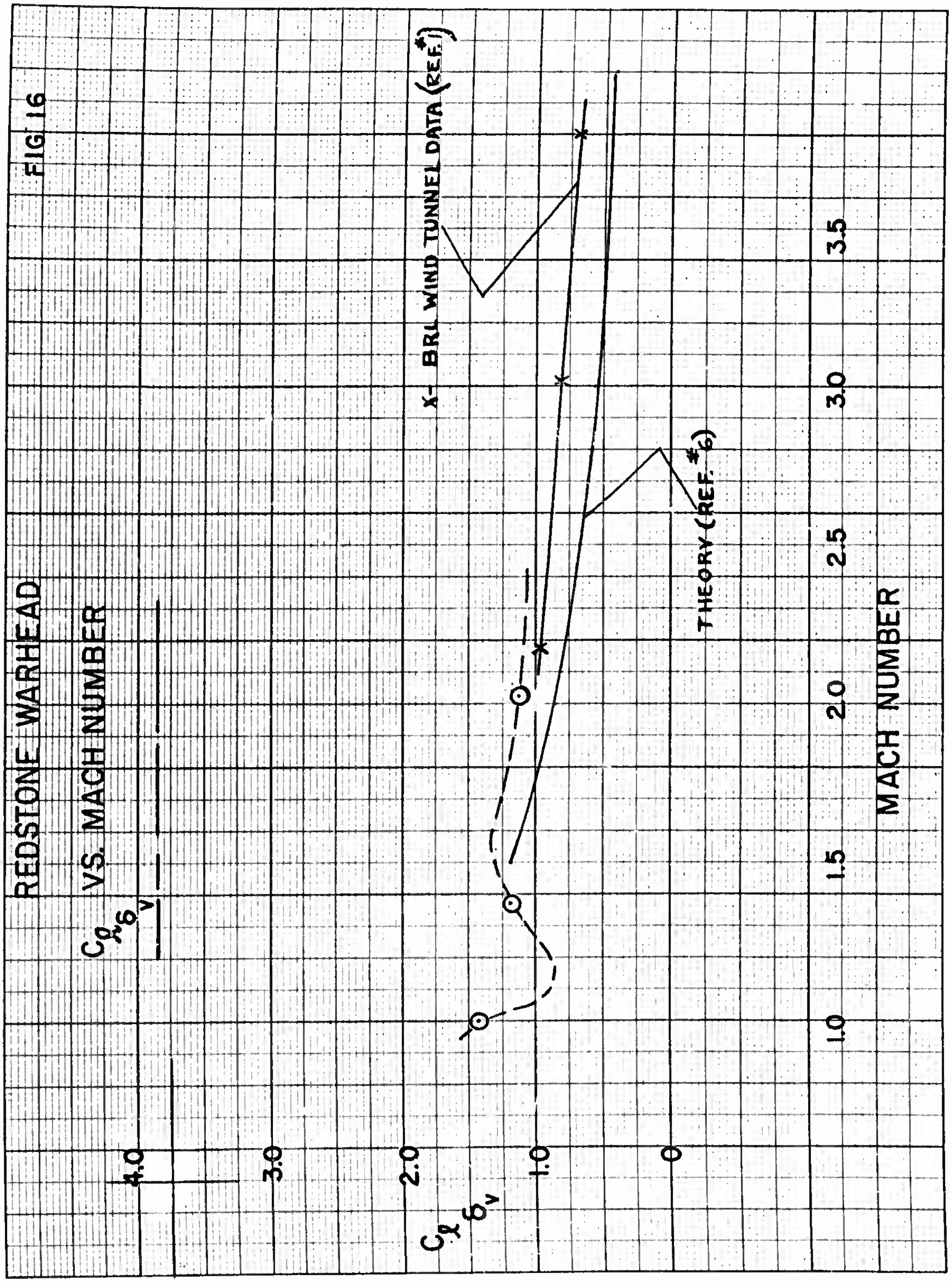
FIG 16
REDSTONE WARHEAD
$C_{l_{\delta_v}}$ VS. MACH NUMBER
X- BRL WIND TUNNEL DATA (REF. #1)
THEORY (REF. #6)
MACH NUMBER
1.0
1.5
2.0
2.5
3.0
3.5
$C_{l_{\delta_v}}$
4.0
3.0
2.0
1.0
0

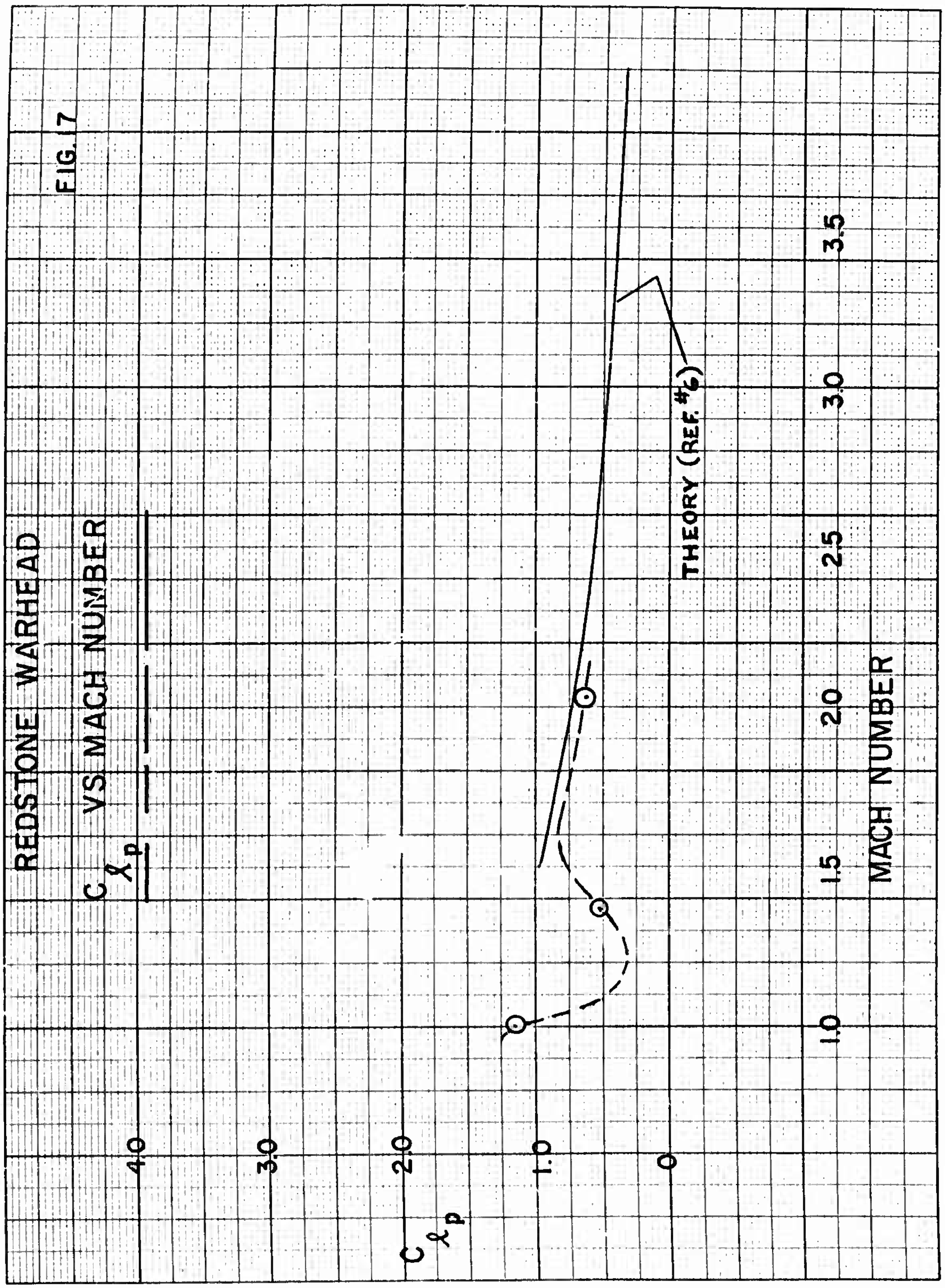
FIG. 17
REDSTONE WARHEAD
C_{ℓ_p} VS MACH NUMBER
THEORY (REF. #6)
C_{ℓ_p}
4.0
3.0
2.0
1.0
0
1.0
1.5
2.0
2.5
3.0
3.5
MACH NUMBER

DISTRIBUTION LIST

No. of Copies	Organization
3	Chief of Ordnance Department of the Army Washington 25, D. C. Attn: ORDTB - Bal Sec (1 cy) ORDTX-AR (1 cy) ORDTU (1 cy)
10	British Joint Services Mission 1800 K Street, N. W. Washington 6, D. C. Attn: Miss Mary Scott, Tech Services
4	Canadian Army Staff 2450 Massachusetts Avenue Washington 8, D. C.
4	Chief, Bureau of Ordnance Department of the Navy Washington 25, D. C. Attn: Re3
2	Commander Naval Proving Ground Dahlgren, Virginia
2	Commander Naval Ordnance Laboratory White Oak Silver Spring, Maryland
2	Commander Naval Ordnance Test Station China Lake, California Attn: Technical Library
2	Commander Naval Air Missile Test Center Point Mugu, California
1	Commanding Officer & Director David W. Taylor Model Basin Washington 7, D. C. Attn: Aerodynamics Laboratory
1	Commander Air Research and Development Command P. O. Box 1395 Baltimore 3, Maryland Attn: Deputy for Development
1	Commander Arnold Engineering Development Center Tullahoma, Tennessee Attn: Deputy Chief of Staff, R&D
3	Director National Advisory Committee for Aeronautics 1512 H Street, N. W. Washington 25, D. C.
2	Director National Advisory Committee for Aeronautics Ames Laboratory Moffett Field, California Attn: Dr. A. C. Charters Mr. H. J. Allen
3	National Advisory Committee for Aeronautics Langley Memorial Aeronautical Laboratory Langley Field, Virginia Attn: Mr. J. Bird Mr. C. E. Brown Dr. Adolf Busemann
1	Chief, Armed Forces Special Weapons Project Washington 25, D. C.
5	Director Armed Services Technical Information Agency Documents Service Center Knott Building Dayton 2, Ohio Attn: DSC - SA

DISTRIBUTION LIST

No. of Copies	Organization	No. of Copies	Organization
4	ASTIA Reference Center Technical Information Div. Library of Congress Washington 25, D. C.	1	Cornell Aeronautical Lab., Inc. Buffalo, New York Attn: Miss Elma T. Evans, Librarian
3	Commanding General Redstone Arsenal Huntsville, Alabama Attn: ORDDW-TMPD, Mr. T. G. Reed	1	Sandia Corp. Sandia Base P. O. Box 5800 Albuquerque, New Mexico Attn: Mr. Wynne K. Cox
3	Commanding Officer Picatinny Arsenal Dover, New Jersey Attn: Samuel Feltman Ammunition Labs.		THRU: Field Manager U. S. Atomic Energy Commission P. O. Box 5900 Albuquerque, New Mexico
1	Commanding General Frankford Arsenal Philadelphia, Penna. Attn: Technical Library	1	Dr. A. E. Puckett Hughes Aircraft Company Florence Avenue at Teal Street Culver City, California
1	Commanding Officer Chemical Corps Chemical & Radiological Laboratory Army Chemical Center, Maryland	1	Dr. C. B. Millikan Guggenheim Aeronautical Lab. California Institute of Technology Pasadena, California
1	Operations Research Office 7100 Connecticut Avenue Chevy Chase, Maryland Washington 15, D. C.		
1	Applied Physics Laboratory 8621 Georgia Avenue Silver Spring, Maryland Attn: Mr. George L. Seielstad THRU: Naval Inspector of Ordnance Applied Physics Lab. 8621 Georgia Avenue Silver Spring, Maryland		

UNCLASSIFIED

UNCLASSIFIED